Matrix Isolation Very Important Paper

DOI: 10.1002/ange.201411234

The Fluorenyl Cation**

Paolo Costa, Iris Trosien, Miguel Fernandez-Oliva, Elsa Sanchez-Garcia, and Wolfram Sander**

In memory of Reiner Sustmann

Abstract: *The fluorenyl cation is a textbook example for a 4π antiaromatic cation. However, contrasting results have been published on how the annelated benzene rings compensate the destabilizing effect of the 4π antiaromatic five-membered ring in its core. Whereas previous attempts to synthesize this cation in superacidic media resulted in undefined polymeric material only, we herein report that it can be generated and isolated in amorphous water ice at temperatures below 30 K by photolysis of diazofluorene. Under these conditions, the fluorenylidene is protonated by water to give the fluorenyl cation, which could be characterized spectroscopically. Its absorption in the visible-light range matches that previously obtained by ultrafast absorption spectroscopy, and furthermore, its IR spectrum could be recorded. The IR bands in amorphous ice very nicely match predictions from DFT and DFT/MM calculations, suggesting the absence of strong interactions between the cation and surrounding water molecules.*

There has been some debate in the literature whether the fluorenyl cation **1** with a formal 4π electron five-membered ring system in its core should be regarded as a prototypical antiaromatic cation, or if the two annelated benzene rings compensate the antiaromaticity, and the molecule is non-aromatic at best or even aromatic.[1–6] In 1980, Olah and Schleyer et al. described unsuccessful attempts to isolate **1** in superacidic media: “We were not able to generate the parent 9-fluorenyl cation 1-H by slowly adding SO_2 or SO_2ClF solutions of possible precursors… at −120 °C. The resulting solutions immediately became dark and unidentifiable polymeric materials were formed”.[7] In contrast, the benzhydryl cation **2** was readily obtained under similar conditions. However, as in **2** the two phenyl groups are rotated out of plane, the higher stability of **2** compared to **1** might reflect a kinetic stabilization of **2** and not the antiaromatic destabilization of **1**. Amyes, Richard, and Novak determined the pK_R values of **1** and **2**, which compare the stabilities of the cations to their respective alcohols, and concluded that “the description of **1** as antiaromatic is misleading because it implies an exceptionally unstable carbocation, and this is not supported by the data”.[1] Schleyer et al. concluded on the basis of calculations of the nucleus-independent chemical shifts (NICS) that the fluorenyl cation **1** is non-aromatic, whereas the fluorenyl anion bearing two more electrons is clearly aromatic.[3]

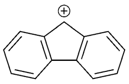
1

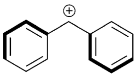
2

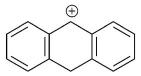
3

An obvious problem when defining the (anti)aromaticity of a molecule is the choice of an appropriate reference system. More O’Ferrall and co-workers selected the planar anthracenyl cation **3** as reference system for **1**, and in very careful experiments, they determined the pK_R value of **1** to be −15.9, that of **2** to be −11.7, and that of **3** to be −5.1.[8] They concluded that **1** is destabilized compared to **3** by 12–13 kcal mol^{-1}. Therefore, the fluorenyl cation **1** is approximately as much destabilized by antiaromaticity as the fluorenyl anion is stabilized by aromaticity. This was confirmed in a later study of Herndon and Mills by calculating the aromatic stabilization energy (ASE) of **1** using various reference systems to be 16.3 ± 1.6 kcal mol^{-1}.[4]

The only available spectroscopic data for **1** are transient absorptions obtained by ultrafast spectroscopy. Mecklenburg and Hilinski observed that the photolysis of fluorenol **4** in H_2O/CH_3OH mixtures produced an absorption at 515 nm with a lifetime of less than 20 ps, which was assigned to **1**.[9] This was later confirmed by McClelland et al.[10] More recently, Platz et al. studied the protonation of fluorenylidene **6** in methanol by picosecond spectroscopy using 9-diazofluorene (**5**) as the precursor (Scheme 1).[11] The same 515 nm transient absorption peak as for **1** was observed, and its lifetime was determined to be only 5 ps. Under similar conditions, the lifetime of benzhydryl cation **2** is 30 ps,[12] which demonstrates the higher reactivity of **1** compared to **2**. In aprotic solvents, laser photolysis of **5** produces singlet fluorenylidene S-**6** ($\lambda_{max} = 420$ nm), triplet fluorenylidene T-**6** ($\lambda_{max} = 470$ nm), and the fluorenyl radical **7** ($\lambda_{max} = 470$, 497 nm).[11]

---

[*] P. Costa, I. Trosien, Prof. Dr. W. Sander
Lehrstuhl für Organische Chemie II
Ruhr-Universität Bochum
44780 Bochum (Germany)
E-mail: wolfram.sander@rub.de

M. Fernandez-Oliva, Dr. E. Sanchez-Garcia
Department of Theory
Max-Planck-Institut für Kohlenforschung
45470 Mülheim an der Ruhr (Germany)
E-mail: esanchez@kofo.mpg.de

[**] This work was supported by the Cluster of Excellence RESOLV (EXC 1069) funded by the Deutsche Forschungsgemeinschaft (DFG). E.S.-G. acknowledges a Liebig Stipend of the Fonds der Chemischen Industrie and support from the Collaborative Research Center SFB 1093 funded by the DFG.

Supporting information for this article is available on the WWW under http://dx.doi.org/10.1002/anie.201411234.

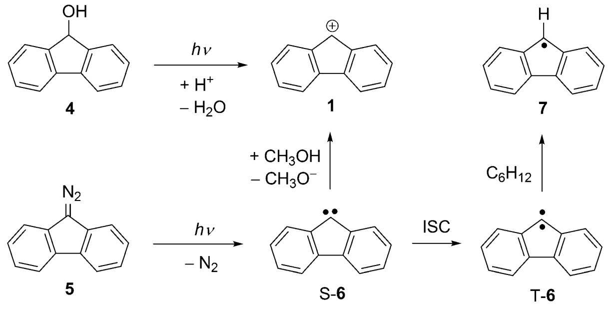

Scheme 1. Generation of fluorenyl cation **1** by protonation of fluorenylidene **6**. ISC = intersystem crossing.

Recently, we found that the benzhydryl cation **2** is kinetically stabilized in amorphous water ice (low-density amorphous ice, LDA ice)[13] at cryogenic temperatures.[14] The photolysis of diphenyldiazomethane, which was matrix-isolated in LDA ice, produced **2** in good yields, which allowed us not only to characterize it by UV/Vis, but also by IR spectroscopy. Although the reaction of **2** with water is highly exothermic, resulting in the pK_R value of -11.7,[8] the reaction with water (or with the hydroxyl ion) leading to the formation of benzhydryl alcohol is only observed at temperatures above 50 K. It was therefore tempting to use the same method to isolate the elusive cation **1** in LDA ice, despite its pK_R value of -15.9 indicating an even lower stability in water.

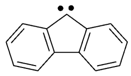
S-**6**

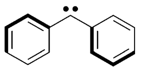
S-**8**

Herein, we describe the reaction of fluorenylidene **6** with water in both H_2O-doped argon matrices and in amorphous water ice. In the first set of experiments, diazofluorene **5** was isolated in argon matrices doped with small amounts (0.5%) of water. UV photolysis (365 nm) at temperatures between 3 K and 10 K produced carbene **6** in its triplet ground state[15] and only traces of reaction products with water. In these matrices, the water molecules are mostly trapped as monomers, as revealed by IR spectroscopy. At temperatures below 20 K, solid argon is very rigid, and the diffusion of water molecules therefore efficiently suppressed. Above 20 K, the matrix becomes softer, and the diffusion of water can be directly monitored by IR spectroscopy:[16–17] Bands of the water dimer and higher oligomers increase in intensity, and all IR bands of T-**6** decrease in intensity. Simultaneously, a new compound with strong absorptions at 714.6, 767.8, 1178.0, and 1600.4 cm^{-1} is formed (Figure 1 b).

When D_2O was used in these experiments, the spectrum of this new species looked virtually identical, and none of its bands showed significant isotopic shifts. Recently, we reported that triplet diphenylcarbene T-**8** reacted with both single molecules of CH_3OH[18] and H_2O[14] to form strongly hydrogen-bonded complexes between the singlet carbene S-**8** and the hydrogen bond donors. We therefore assign the new species formed in the reaction between T-**6** and H_2O to the singlet carbene complex S-**6**$\cdots H_2O$.

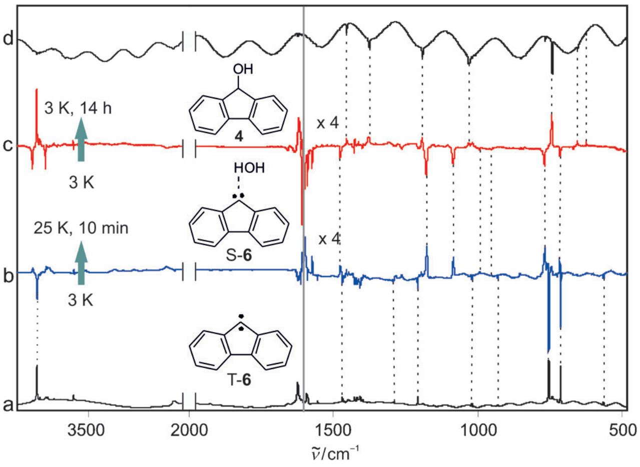

Figure 1. IR spectra showing the chemistry of fluorenylidene **6** in H_2O doped (0.5%) argon. a) T-**6** obtained after photolysis of **5** at 3 K. b) Difference IR spectrum of the same matrix after annealing at 25 K for 10 minutes. Bands pointing downwards, which were assigned to T-**6** and H_2O, are disappearing, bands pointing upwards, which were assigned to the complex between S-**6** and H_2O, are appearing. c) Difference IR spectrum at 3 K after 14 hours. Bands pointing upwards were assigned to 9-fluorenol **4** and are appearing, bands pointing downwards correspond to S-**1**$\cdots H_2O$ and are disappearing. d) Compound **4** in argon at 3 K.

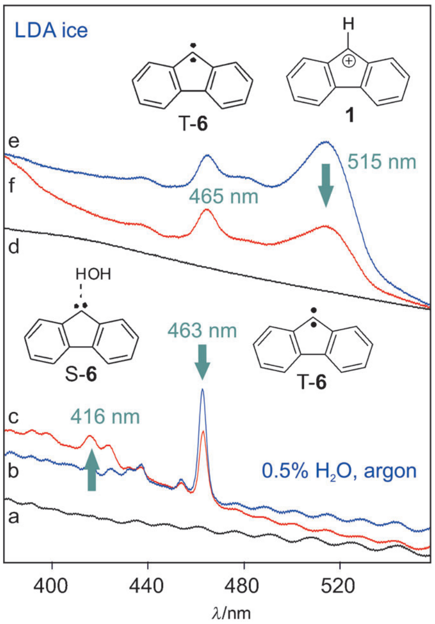

Figure 2. Visible spectra showing the photochemistry of diazofluorene **5** in H_2O doped (0.5%) argon (bottom) and LDA water ice (top). a) Spectrum after deposition of **5** in argon/H_2O (0.5%) at 8 K. b) On irradiation ($\lambda = 365$ nm) for 1 hour, T-**6** was formed with $\lambda_{max} = 463$ nm. c) On annealing at 25 K for 10 min, the amount of T-**6** decreased, and S-**6**$\cdots H_2O$ ($\lambda_{max} = 416$ nm) was formed. d) Spectrum after deposition of **5** in LDA water ice at 8 K. e) On irradiation ($\lambda = 365$ nm) for 10 min, T-**6** ($\lambda_{max} = 465$ nm) and cation **1** ($\lambda_{max} = 515$ nm) were formed. f) On irradiation ($\lambda = 520$ nm) for 10 min, the absorption of **1** at 515 nm decreased in intensity.

This assignment was confirmed by following the reaction by UV/Vis spectroscopy (Figure 2b,c). The characteristic absorption of T-**6** at 463 nm decreased in intensity during annealing of the matrix at 25 K, and a new band with a maximum at 416 nm appeared, nicely matching the transient absorption at 420 nm observed for S-**6** in picosecond absorption spectroscopy (Supporting Information, Figure S1).[11] The reaction of T-**6** with H_2O was also studied by EPR spectroscopy. After annealing for five minutes at 25 K, the intensity of the triplet signal of T-**6** had already decreased by 59% without formation of new paramagnetic species.

The strongly basic singlet state S-**6** forms a strong hydrogen bond with water whereas T-**6** only weakly interacts. The additional stabilization of S-**6** by hydrogen bonding is larger than the S–T gap, and therefore, the singlet state becomes the ground state. This was confirmed by ab initio calculations (CCSD(T)/cc-pVDZ//B3LYP-D3/def2-TZVP), which predicted an S–T gap of 3.4 kcal mol^{-1} for **6** (in the gas phase). In the complex with water, this gap is inverted to -1.1 kcal mol^{-1} in favor of the singlet.

The complex S-**6**$\cdots H_2O$ is only metastable, and even at 3 K, it slowly rearranges to fluorenol **4** (Figure 1d, Scheme 2). At 3 K and at 12 K, almost identical rates of $1.3\pm0.2\times10^{-5}\,\text{s}^{-1}$ were recorded for this rearrangement. This implies that the thermal activation barrier is zero, indicating a tunneling mechanism. With D_2O, only a small kinetic isotope effect of approximately 2 was found, and therefore, the hydrogen atom transfer cannot be the rate-determining step. The activation barrier for the thermal rearrangement was calculated to be 9.3 kcal mol^{-1} (CCSD(T)/cc-pVDZ//B3LYP-D3/def2-TZVP, see the Supporting Information), which is prohibitively high for any thermal reaction at 3 K, and again strongly supports a tunneling mechanism. The calculations suggest that in the gas phase and in argon, the ion pair is not a stationary point, and that the formation of **4** from S-**6**$\cdots H_2O$ is a concerted process.

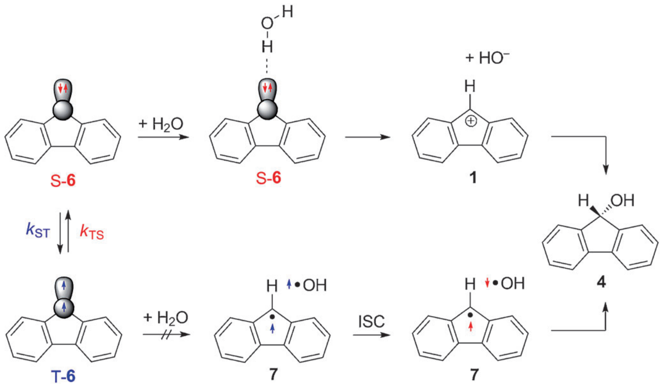

Scheme 2. Reaction of fluorenylidene **6** with H_2O.

So far, the reaction of fluorenylidene **6** with water is analogous to that of diphenylcarbene **8** with water.[14] The crucial question is whether or not LDA water ice is able to protonate carbene **6** to form the destabilized fluorenyl cation **1**. Photolysis ($\lambda = 365$ nm) of **5** in LDA ice at 8 K resulted in two new absorptions in the visible region of the spectrum (Figure 2e): a band with $\lambda_{max} = 515$ nm that exactly matches the reported picosecond transient absorption of cation **1**,[10–11] and a band with $\lambda_{max} = 465$ nm that fits to the visible absorption of T-**6**. The EPR spectrum shows the characteristic triplet spectrum of T-**6**, which demonstrates that in LDA ice, **6** has a triplet ground state, and that the singlet complex S-**6**$\cdots H_2O$ is not formed under these conditions (see the Supporting Information).

To confirm these assignments, we also monitored the photolysis (365 nm) of **5** in LDA ice at 3 K by IR spectroscopy (Figure 3). A major product found after the photolysis was fluorenol **4**, which could be identified by comparison with an authentic sample isolated in LDA ice. In addition, a new compound with strong IR absorptions at 1575.7 and 1076.8 cm^{-1} and medium-intensity absorptions at 1343.7 and 1163.5 cm^{-1} was observed (Figure 3, Table 1). When D_2O was used in these experiments, the band at 1343.7 cm^{-1} showed a pronounced isotopic shift of $-19.8\,\text{cm}^{-1}$, which clearly indicates that deuterium was incorporated into the new compound. Warming the LDA matrix from 3 K to 50 K resulted in the disappearance of all of these absorptions and the formation of **4**. We therefore assign the new compound to fluorenyl cation **1**. The IR frequencies, relative intensities, and isotopic shifts of **1** and [D]-**1** calculated at the B3LYP level of theory (Figure 3c,e) are in excellent agreement with the experimental data (Figure 3a,d) and nicely support our assignment of **1**.

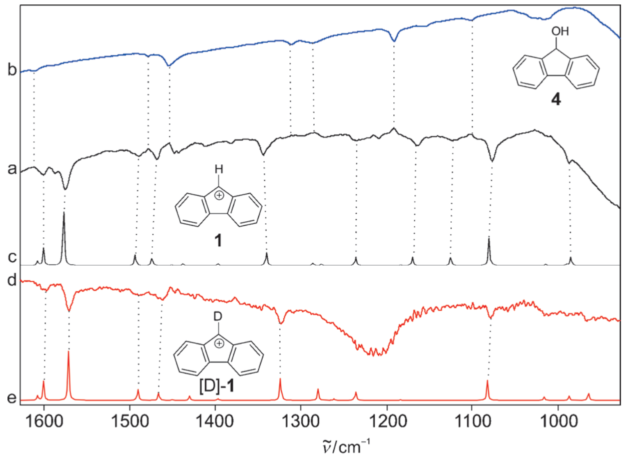

Figure 3. IR spectra showing the photochemistry of diazofluorene **5** in LDA water ice. The fluorenyl cation **1** was generated by UV photolysis (365 nm) for 15 min at 9 K. a) Difference IR spectrum showing changes in the matrix after annealing for several minutes at 50 K. Bands pointing downwards are disappearing and were assigned to **1**, bands pointing upwards are increasing in intensity and were assigned to **4**. b) Fluorenol **4** isolated in LDA ice at 9 K. c) Calculated IR spectrum of **1**, B3LYP-D3/def2-TZVP scaled by 0.977. d) Same conditions as described in (a) but using D_2O LDA ice, showing the formation of [D]-**1**. e) Calculated IR spectrum of [D]-**1**, B3LYP-D3/def2-TZVP scaled by 0.977.

LDA water ice has proven to be a suitable medium to isolate unstable carbenium ions, and for the first time, cation

Table 1: IR spectroscopic data of the fluorenyl cation **1** and its deuterated isotopomer [D]-**1** matrix-isolated in LDA water ice compared to calculated data.

	Calculated for the gas phase[a]		QM/MM[b]	LDA ice[c]		
Nr.	$\tilde{\nu}$ [cm^{-1}] (shift)[d]	I_{rel} ([D]-**1**)[e]	$\tilde{\nu}$ [cm^{-1}]	$\tilde{\nu}$ [cm^{-1}] (shift)[d]	I_{rel} ([D]-**1**)[e]	Assignment
26	1008.8	16	992.9	986.0	13	δ_{ip}(C−H)
32	1106.8 (+2.1)	51 (40)	1081.4	1076.8 (+1.7)	52 (57)	δ_{ip}(C−H)
34	1152.8	15	1121.2	1117.2	13	δ_{ip}(C−H)
35	1198.6	16	1169.0	1163.5	26	δ_{ip}(C−H)
38	1267.0	14	1245.4	1235.1	14	δ_{ip}(C−H)
42	1373.4 (−16.4)	24 (44)	1362.4	1343.7 (−19.8)	30 (50)	ν_{as}(C−C−C)
46	1510.8 (−8.3)	13 (15)	1490.3	1469.0 (−7.3)	17 (23)	δ_{ip}(C−H)
47	1530.7 (−3.2)	20 (22)	1521.9	1490.5 (−1.0)	13 (14)	ν(C=C)
48	1616.8 (−6.4)	100 (100)	1613.4	1575.7 (−4.4)	100 (100)	ν(C=C)
50	1640.9 (0.0)	33 (39)	1620.7	1601.2 (−4.0)	13 (29)	ν(C=C)

[a] B3LYP-D3/def2-TZVP calculation in the gas phase. [b] B3LYP-D3/def2-TZVP//CHARMM calculation of **1** in a water box. [c] LDA ice at 9 K. [d] Deuterium isotopic shift of [D]-**1** relative to **1** in parentheses. [e] Relative intensity of the [D]-**1** isotopomer in parentheses. as = asymmetric, δ_{ip} = in-plane deformation, ν = stretch.

1 could be isolated and kinetically stabilized in condensed phase. This is remarkable as the reaction of **1** with water is highly exothermic, and in protic solvents, its lifetime of only a few picoseconds is extremely short. Obviously, below 30 K, the reaction of **1** with surrounding water molecules or with the hydroxyl ion does not occur, and even at 50 K, the reaction is slow. We speculate that after its formation, the hydroxyl ion very efficiently migrates away from the cation by fast proton exchange in the hydrogen bond network. The energy necessary for this could be provided by the excess energy released after photolysis of precursor **5** or by the exothermic protonation of **6**.

The IR spectrum of **1** nicely matches the spectrum predicted by DFT calculations in the gas phase. Apart from some line-broadening, presumably caused by the inhomogeneity of the amorphous ice, there are no significant shifts that could indicate strong interactions with the surrounding water molecules. This was confirmed by quantum mechanical/molecular mechanical (QM/MM) calculations using the same DFT method as in the gas phase, but including a box of explicit water molecules to simulate solvation effects (Table 1). These calculations suggest that the QM cation **1** is only weakly interacting with the surrounding MM water molecules, and consequently, only modest solvent-induced red-shifts of the IR bands of **1** are predicted. The QM/MM predicted IR frequencies are in almost perfect agreement with the experimental data, demonstrating the validity of the theoretical model. In summary, LDA ice is an ideal, only weakly interacting medium of low polarity to isolate and characterize highly reactive cations.

Experimental Section

Matrix-isolation spectroscopy: Matrix-isolation experiments were performed by standard techniques using Sumitomo Heavy industries two-staged closed-cycle helium cryostats (cooling power 1 W at 4 K) to obtain temperatures of approximately 3 K. Water was degassed several times before deposition. The matrices were generated by co-deposition of diazofluorene **5** and 0.5 % of water with a large excess of argon (Messer Griesheim, 99.99 %) on top of different substrates (Cu rod, CsI, and sapphire windows, respectively for EPR, FT-IR, and UV/Vis spectroscopy) cooled to 3 K. A flow rate of approximately 1.80 sccm was used for the deposition of the matrix. Fluorenylidene T-**6** was generated by photolysis of **5** at 3 K using an LED source ($\lambda = 365$ nm). After annealing at 25 K for 10 minutes, the matrices were cooled back to 3 K. LDA ice matrices were generated by slow deposition of water at 50 K followed by cooling to 3–10 K. FT-IR spectra were recorded from 400 to 4000 cm^{-1} with 0.5 cm^{-1} resolution. Matrix EPR spectra were recorded using a Bruker ELEXSYS 500 X-band spectrometer. Matrix UV/Vis spectra were recorded with a Varian Cary 5000 spectrometer in the range of 200–800 nm with a resolution of 0.1 nm.

Computational methods: All gas-phase DFT geometry optimizations and frequency calculations were carried out using the B3LYP functional[19] with the D3 empirical dispersion correction[20] and the def2-TZVP basis set. The TURBOMOLE program (v. 6.4)[21,22] was employed. CCSD(T) single-point calculations were performed using the cc-pVDZ basis set[23] and the MOLPRO program.[24,25] QM MD, QM/MM MD simulations and QM/MM optimizations were performed using the program ChemShell[26] as an interface to TURBOMOLE 6.4 and CHARMM 31b1.[27] QM MD simulations were conducted at the B3LYP-D3/def2-SVP level of theory whereas QM/MM MD simulations were carried out at the B3LYP-D3/def2-SVP//CHARMM level of theory. For more details, see the Supporting Information.

Received: November 19, 2014

Keywords: antiaromaticity · carbenium ions · IR spectroscopy · matrix isolation · QM/MM calculations

[1] T. L. Amyes, J. P. Richard, M. Novak, *J. Am. Chem. Soc.* **1992**, *114*, 8032 – 8041.

[2] C. F. Rodriquez, D. L. Vuckovic, A. C. Hopkinson, *J. Mol. Struct.: THEOCHEM* **1996**, *363*, 131 – 138.

[3] H. Jiao, P. v. R. Schleyer, Y. Mo, M. A. McAllister, T. T. Tidwell, *J. Am. Chem. Soc.* **1997**, *119*, 7075 – 7083.

[4] W. C. Herndon, N. S. Mills, *J. Org. Chem.* **2005**, *70*, 8492 – 8496.

[5] N. S. Mills, K. B. Llagostera, C. Tirla, S. M. Gordon, D. Carpenetti, *J. Org. Chem.* **2006**, *71*, 7940 – 7946.

[6] S. Pogodin, I. Agranat, *J. Org. Chem.* **2007**, *72*, 10096 – 10107.

[7] G. A. Olah, G. K. S. Prakash, G. Liang, P. W. Westerman, K. Kunde, J. Chandrasekhar, P. V. R. Schleyer, *J. Am. Chem. Soc.* **1980**, *102*, 4485 – 4492.

[8] M. C. Courtney, A. C. MacCormack, R. A. M. O'Ferrall, *J. Phys. Org. Chem.* **2002**, *15*, 529 – 539.

[9] S. L. Mecklenburg, E. F. Hilinski, *J. Am. Chem. Soc.* **1989**, *111*, 5471 – 5472.

[10] R. A. McClelland, N. Mathivanan, S. Steenken, *J. Am. Chem. Soc.* **1990**, *112*, 4857 – 4861.

[11] J. Wang, J. Kubicki, E. F. Hilinski, S. L. Mecklenburg, T. L. Gustafson, M. S. Platz, *J. Am. Chem. Soc.* **2007**, *129*, 13683 – 13690.

[12] J. Peon, D. Polshakov, B. Kohler, *J. Am. Chem. Soc.* **2002**, *124*, 6428 – 6438.

[13] M. S. Gudipati, *J. Phys. Chem. A* **2004**, *108*, 4412 – 4419.

[14] P. Costa, M. Fernandez-Oliva, E. Sanchez-Garcia, W. Sander, *J. Am. Chem. Soc.* **2014**, *136*, 15625 – 15630.

[15] G. A. Bell, I. R. Dunkin, *J. Chem. Soc. Faraday Trans. 2* **1985**, *81*, 725 – 734.

[16] A. Mardyukov, R. Crespo-Otero, E. Sanchez-Garcia, W. Sander, *Chem. Eur. J.* **2010**, *16*, 8679 – 8689.

[17] W. Sander, S. Roy, I. Polyak, J. M. Ramirez-Anguita, E. Sanchez-Garcia, *J. Am. Chem. Soc.* **2012**, *134*, 8222 – 8230.

[18] P. Costa, W. Sander, *Angew. Chem. Int. Ed.* **2014**, *53*, 5122 – 5125; *Angew. Chem.* **2014**, *126*, 5222 – 5225.

[19] A. D. Becke, *J. Chem. Phys.* **1993**, *98*, 5648 – 5652.

[20] S. Grimme, J. Antony, S. Ehrlich, H. Krieg, *J. Chem. Phys.* **2010**, *132*, 154104.

[21] R. Ahlrichs, M. Bär, M. Häser, H. Horn, C. Kölmel, *Chem. Phys. Lett.* **1989**, *162*, 165 – 169.

[22] TURBOMOLE V6.4 2012, a development of the University of Karlsruhe and Forschungszentrum Karlsruhe GmbH, 1989 – 2007, TURBOMOLE GmbH, since 2007; available from http://www.turbomole.com.

[23] T. H. Dunning, *J. Chem. Phys.* **1989**, *90*, 1007 – 1023.

[24] H.-J. Werner, P. J. Knowles, G. Knizia, F. R. Manby, M. Schütz, *Wiley Interdiscip. Rev.: Computational Mol. Sci.* **2012**, *2*, 242 – 253.

[25] MOLPRO, version 2012.1, a package of ab initio programs, H.-J. Werner, P. J. Knowles, G. Knizia, F. R. Manby, M. Schütz, P. Celani, T. Korona, R. Lindh, A. Mitrushenkov, G. Rauhut, K. R. Shamasundar, T. B. Adler, R. D. Amos, A. Bernhardsson, A. Berning, D. L. Cooper, M. J. O. Deegan, A. J. Dobbyn, F. Eckert, E. Goll, C. Hampel, A. Hesselmann, G. Hetzer, T. Hrenar, G. Jansen, C. Köppl, Y. Liu, A. W. Lloyd, R. A. Mata, A. J. May, S. J. McNicholas, W. Meyer, M. E. Mura, A. Nicklass, D. P. O'Neill, P. Palmieri, D. Peng, K. Pflüger, R. Pitzer, M. Reiher, T. Shiozaki, H. Stoll, A. J. Stone, R. Tarroni, T. Thorsteinsson, M. Wang, see http://www.molpro.net.

[26] P. Sherwood, A. H. de Vries, M. F. Guest, G. Schreckenbach, C. R. A. Catlow, S. A. French, A. A. Sokol, S. T. Bromley, W. Thiel, A. J. Turner, S. Billeter, F. Terstegen, S. Thiel, J. Kendrick, S. C. Rogers, J. Casci, M. Watson, F. King, E. Karlsen, M. Sjøvoll, A. Fahmi, A. Schäfer, C. Lennartz, *J. Mol. Struct.: THEOCHEM* **2003**, *632*, 1 – 28.

[27] B. R. Brooks, C. L. Brooks, A. D. Mackerell, L. Nilsson, R. J. Petrella, B. Roux, Y. Won, G. Archontis, C. Bartels, S. Boresch, A. Caflisch, L. Caves, Q. Cui, A. R. Dinner, M. Feig, S. Fischer, J. Gao, M. Hodoscek, W. Im, K. Kuczera, T. Lazaridis, J. Ma, V. Ovchinnikov, E. Paci, R. W. Pastor, C. B. Post, J. Z. Pu, M. Schaefer, B. Tidor, R. M. Venable, H. L. Woodcock, X. Wu, W. Yang, D. M. York, M. Karplus, *J. Comput. Chem.* **2009**, *30*, 1545 – 1614.